

Unifying Bilateral Filtering and Adversarial Training for Robust Neural Networks

Neale Ratzlaff, Fuxin Li

School of Electrical Engineering and Computer Science
Oregon State University
ratzlafn@oregonstate.edu, lif@eecs.oregonstate.edu

Abstract. Recent analysis of deep neural networks has revealed their vulnerability to carefully structured adversarial examples. Many effective algorithms exist to craft these adversarial examples, but performant defenses seem to be far away. In this work, we explore the use of edge-aware bilateral filtering as a projection back to the space of natural images. We show that bilateral filtering is an effective defense in multiple attack settings, where the strength of the adversary gradually increases. In the case of adversary who has no knowledge of the defense, bilateral filtering can remove more than 90% of adversarial examples from a variety of different attacks. To harden our network against an adversary with complete knowledge of our defense, we adapt the bilateral filter as a trainable layer in a neural network. When trained under a framework of robust optimization, we show that the resulting model is hard to fool with even the best attack methods.

1 Introduction

Deep neural networks have achieved outstanding performance in the fields of computer vision, text processing, and speech recognition. However, it has been shown that they are vulnerable to targeted perturbations added to benign inputs. The perturbed inputs, known as *adversarial examples*, can cause a classifier to output highly confident, but incorrect predictions. Adversarial examples are cheap to create, and defending against them is still an open problem.

The majority of prior work has studied adversarial examples in the context of computer vision, where they pose the clearest threat. Small perturbations, imperceptible to humans, can be added to input images that cause a classifier to output false predictions. Because of the particular success of neural networks in computer vision, these models are being deployed in areas like autonomous driving, facial recognition, and malware detection. Recent work has shown that these systems are vulnerable in the real world to adversarial examples [9], which makes the problem of resisting adversarial attacks a growing concern.

Many attacks and defenses have been proposed, and there has emerged two central methods for defending against adversarial examples. *Denoising* approaches attempt to remove the adversarial perturbations from the inputs as a preprocessing step. This is often done by filtering, or by projecting the input to

a lower dimensional space that cannot represent high frequency perturbations [28,30]. These methods often give high accuracy, even on difficult datasets like ImageNet. But it has been shown that an attacker with knowledge of the defense can successfully circumvent them [2].

On the other hand, *Adversarial training* methods uses principles from robust optimization to train models which resist adversarial attacks. Under the adversarial training framework, adversarial examples are combined with the natural training set to increase the model’s robustness to attack. These methods are expensive: requiring many more training examples, and have not been shown to scale well to natural image datasets like ImageNet.

In this work we propose a method which combines denoising and robust optimization approaches, and yields a classifier which can defend well against adversarial examples while preserving accuracy on clean inputs. In particular, we study the application of the bilateral filter to the problem of recovering the clean inputs from adversarial examples. Bilateral filtering is a well-used approach in computer vision to edge-aware nonlocal smoothing. We show that a nonlinear Gaussian filter such as the bilateral filter is able to reliably remove adversarial perturbations from inputs. We have found that, with appropriate parameters, bilateral filtering can recover 99% of the adversarial images so that a classifier can predict the original label. We then introduce BFNet: an end-to-end model incorporating a differentiable bilateral filtering layer. We show that BFNet is naturally robust to attacks from many first order adversaries, greatly reducing the strength of both L_∞ and L_2 attacks. When combined with adversarial training, we achieve state of the art results on MNIST and CIFAR10. Our method works with zero knowledge of either the network or any incoming attack, making it applicable to a variety of models and datasets. We demonstrate the versatility of our method by testing bilateral filter based defenses in three different attack settings.

1. Against adversaries with no knowledge of our defense, we show that a vanilla bilateral filter with fixed parameters can reliably remove adversarial perturbations created by a variety of strong adversaries.
2. We further develop an adaptive filtering network which predicts bilateral filter parameters from an input image, to combat an adversary who employs a larger attack repertoire. We test our network on the ImageNet dataset, using Inception V3 and InceptionResNet V2 classifiers. We found that our adaptive filtering network successfully removes adversarial perturbations from natural images, recovering the clean class label.
3. The strongest adversary has access to our defense, and can optimize against it. We show that BFNet is naturally robust to such perfect-knowledge attacks on ImageNet. We also combine BFNet with adversarial training to further increase its resistance to attack. In particular, we evaluated the ability of adversaries to attack our network on the MNIST and CIFAR10 datasets, and achieve state of the art results for PGD and FGSM attacks.

2 Related Work

2.1 Adversarial Attacks

There have been many proposed attacks for creating adversarial examples. We give a brief description of the six attacks that we used to test our models.

A. Projected Gradient Descent (PGD)

When measuring the robustness of a model to adversarial attack. It is helpful to limit the strength of the adversary by generating perturbations within a bounded magnitude ϵ . In [18,19], generating an adversarial example is the task of solving the objective:

$$\max_{\delta \leq \epsilon} L(\theta, x + \delta, y_{true})$$

PGD is used to minimize this objective under a loss function L , yielding an image with perturbations with magnitude less than ϵ with respect to the max norm, and achieves the highest possible loss.

B. Fast Gradient Sign Method (FGSM)

FGSM [10] is a one step linearization of the above objective. FGSM finds adversarial examples by assuming linearity at the decision boundary. Given an image x , we find a perturbation η under the max norm:

$$\eta = \epsilon \cdot \text{sign}(\nabla_x L(\theta, x, y))$$

Where θ is the parameters of the network, y is the original label, and L is the loss function used to train the network.

C. Momentum Iterative Method

The Momentum Iterative Fast Sign Gradient Method (MI-FGSM) [7] is an iterative version of the FGSM attack. MI-FGSM moves pixel values linearly along the gradient toward the decision boundary. MI-FGSM improves on FGSM by introducing a momentum term into gradient calculation.

$$g_{t+1} = \mu \cdot g_t + \frac{\nabla_x L(x_t^*, y)}{\|\nabla_x L(x_t^*, y)\|_1}$$

The gradient is then used to iteratively update the image

$$x_{t+1}^* = x_t^* + \alpha \cdot (g_{t+1})$$

The authors claim that simply using an iterative FGSM leads to greedy overfitting of the decision boundary, and thus falls into local poor maxima. Adding momentum stabilizes the update direction and creates a stronger adversarial example.

D. L-BFGS-B

[31] used box-constrained L-BFGS to generate adversarial examples with minimal distortion under the L_2 norm. Given a natural image x and a target class y_{true} , the adversarial objective is as follows

$$\min \left[c \cdot \|x - (x + \delta)\|_2^2 + L(x + \delta, y_{target}) \right]$$

Where δ is the adversarial perturbation, L is the loss function, and the parameter c controls the trade-off between the magnitude and strength of the perturbation.

E. Carlini & Wagner Attack (L_2)

[4] proposed three iterative attacks which create adversarial examples under the L_0 , L_2 , and L_∞ norms. In this work we consider the most powerful attack, the white-box L_2 attack. Specifically, they minimize

$$\min \left\| \frac{1}{2}(\tanh(w) + 1)x \right\|_2^2 + cf\left(\frac{1}{2}(\tanh(w) + 1)\right)$$

$$\text{Where } f(x') = \max(\max\{Z_i(x') : i \neq t\}Z_t(x'), -\kappa)$$

Here, t is the target label, Z refers to the logits of the network, κ controls the confidence of the new classification, and the $\frac{1}{2} \tanh$ term constrains the result to pixel space.

F. DeepFool

Deepfool is an iterative, first order method used to find minimal distortion under the L_2 norm [22]. Deepfool linearizes the classifier itself and performs gradient descent until the image is misclassified. The DeepFool objective is as follows:

$$\min_{\delta} \|\delta\|_2 \quad \text{subject to} \quad \operatorname{argmax} f(x) \neq \operatorname{argmax} f(x + \delta)$$

In addition to the attacks listed above, other methods have been proposed. L_0 attacks such as [27] choose to measure adversarial perturbations by the minimum change necessary to produce an incorrect prediction.

2.2 Adversarial Defenses

There is a growing body of work concerning defense against adversarial attacks [24,26,36,16]. Many of these lay an important foundation for our method. JPEG compression was studied in [8,14,6], and was found to be effective at removing adversarial perturbations. However, the JPEG encoding operations are not differentiable. Leaving open the question of robustness to direct attack, where the adversary has knowledge of the defense and seeks to counter it. We improve on this method by introducing a fully differentiable defense, and showing that it is robust to direct attack.

Other recent defenses attempt to remove adversarial perturbations by projecting inputs back onto the real data manifold [20]. [30] projects inputs using a generative adversarial network. Given a normal or adversarial image, a generator is trained to produce a image from the normal data distribution. This method also does not test against direct attack, and has been shown to be successfully fooled by the CW attack [3]. Our method can also be seen as a projection back to the data manifold, where we impose the constraint that the resulting image must be piecewise smooth. Again, we show our method to remain effective under direct attack.

On the other hand, adversarial training methods [10,19,29,32] combine adversarial examples with the natural training set to increase the model’s robustness to adversarial attack. These methods are promising as they attempt provide a guarantee on both the type of adversary and the magnitude of the perturbation they are resistant to. In practice however, these methods are hard to scale as they require expensive computation in the inner training loop to generate adversarial examples. When training on a large dataset like ImageNet, generating a sufficient amount of strong adversarial examples can be intractable. This problem has been mitigated by training against a weak adversary like FGSM [32] which can quickly generate adversarial examples. But training models that are robust to strong adversaries on ImageNet or Cifar10 is still an open problem.

3 Methods

In this section we present our motivation for using a bilateral filter as the building block for our robust defenses. We give a quick discussion of the theory of edge aware filtering and how it applies to adversarial examples. We show that it can remove adversarial perturbations crafted by many strong attacks. We then describe our end to end approach for training a classifier with a bilateral filter as a differentiable filtering layer. Finally, we recognize the current state of the art method for training models robust to adversarial attacks, adversarial training, and we show that our method can extend adversarial training to create still more robust models.

Existing adversarial attacks fool deep networks by exploiting the training distribution: creating inputs which lie very close to decision boundaries. An effective defense would be to project the perturbed image back to a distribution similar to the training distribution. But it is not so clear what type of projection we should employ. We observe that gradients in natural images are often *piecewise-smooth*. In contrast, adversarial attacks perturb images such that the resulting gradients are locally non-smooth with respect to the perturbed components of the image. A nonlinear Gaussian filter like the bilateral filter can be viewed as a projection back to the distribution of piecewise-smooth functions. The bilateral filter preserves local discontinuities (edges), while smoothing image gradients, for this reason the bilateral filter is a natural candidate projection for removing adversarial perturbations.

By design, the perturbations in adversarial images have very small magnitudes, such that these perturbations are imperceptible to humans. In the case of multi-step attacks, the L_∞ or L_2 distance can be small enough that any blurring filter will destroy the perturbation. Indeed it has been shown in prior work that projection based methods are enough to remove perturbations from adversarial inputs. However, as prior work did not examine performance under perfect-knowledge attacks, we cannot be sure of their reliability. On the other hand, bilateral filters can be formulated as a differentiable operation within a DNN and trained end to end. This new network, which we call BFNet, can be validated against perfect-knowledge adversarial attacks to test its robustness.

3.1 Threat Model

Prior work often presents adversarial attacks and defenses as being either a white-box or black-box attack. In the white-box threat model, the attacker has full access to training data, model parameters and architecture. The black-box threat model considers the case where the attacker has little to no knowledge about the model architecture, parameters, or training data. In the most restrictive setting, the attack may only have access to the argmax output of a softmax operation. In this work we consider white-box attacks, as they are categorically stronger adversaries than black-box attacks. We consider three different levels of robustness for our bilateral filter defenses. We measure robustness against an attacker without knowledge of the defense, a changing attacker who may employ many different adversarial attacks, and finally an adversary who can mount a perfect-knowledge attack.

3.2 The Bilateral Filter

The bilateral filter is a non-linear Gaussian filter that is used to smooth non-local image gradients, while preserving sharp edges. Similar to other Gaussian filters, the bilateral filter replaces pixel values with a weighted average of the neighboring intensity values. Edges are preserved through weighting both pixel-wise Euclidean distance as well as differences in range, intensity, depth, etc. For an image I , window Ω centered at pixel p , the bilateral filter is formulated as a domain function G_s , and a range function G_r :

$$I_{filtered}(p) = \frac{1}{W_p} \sum_{q \in \Omega} G_s(\|\mathbf{p} - \mathbf{q}\|) G_r(I_p - I_q) I_q$$

Where the normalization term W_p is:

$$W_p = \sum_{q \in \Omega} G_s(\|\mathbf{p} - \mathbf{q}\|) G_r(I_p - I_q)$$

Each neighboring pixel is assigned a weight according to both spatial closeness and value difference. To calculate the resulting weight on a single pixel (i, j) and

its neighbor (k, l) , then the weight assigned to (k, l) is as follows:

$$w(i, j, k, l) = \exp \left(- \frac{(i - k)^2 + (j - l)^2}{2\sigma_s^2} - \frac{\|I(i, j) - I(k, l)\|^2}{2\sigma_r} \right)$$

where σ_s and σ_r are parameters which control the strength of the domain and range functions respectively. The value of the filtered pixel is given after normalization:

$$I_p(i, j) = \frac{\sum_{k, l} I(k, l) w(i, j, k, l)}{\sum_{k, l} w(i, j, k, l)}$$

We use this bilateral filter as the instrument by which we defend against the naive adversary.



Fig. 1: The effect of filtering on a L-BFGS-B adversarial image. (a) is the original adversarial image, (b) is the image after 3x3 bilateral filtering and (c) is the image after 3x3 average pooling. The bilateral filter is superior when removing small perturbations while preserving the underlying class features

To test the efficacy of the bilateral filter to recover clean inputs from adversarial examples, we generated a set of adversarial examples from a range of powerful adversaries. Our first approach was to manually tune parameters for each input image, to test the effective range of parameters which could recover the original label from an adversarial example. We found that with carefully chosen parameters, the corrupted labels could indeed be recovered. Our experiments showed that the small perturbations created by iterative methods like the Carlini & Wagner attack and DeepFool were easier to remove with a bilateral filter than the larger perturbations created with one step attacks. To remove perturbations generated by iterative attacks, we used small kernels 3 - 5 pixels wide, and σ_s , σ_r values of 0.5. Stronger filtering offers no benefit, as the resulting images from iterative attacks have imperceptible perturbations which are removed with light filtering. One step attacks perturb every pixel in the image with the same magnitude of noise. As a result, we increased kernel width to 7 and σ_s to 3, holding σ_r constant. These parameters reliably removed adversarial perturbations from L_∞ attacks with a bounded distance of 0.3, as well as unbounded L_2 attacks. The results can be found in table 1

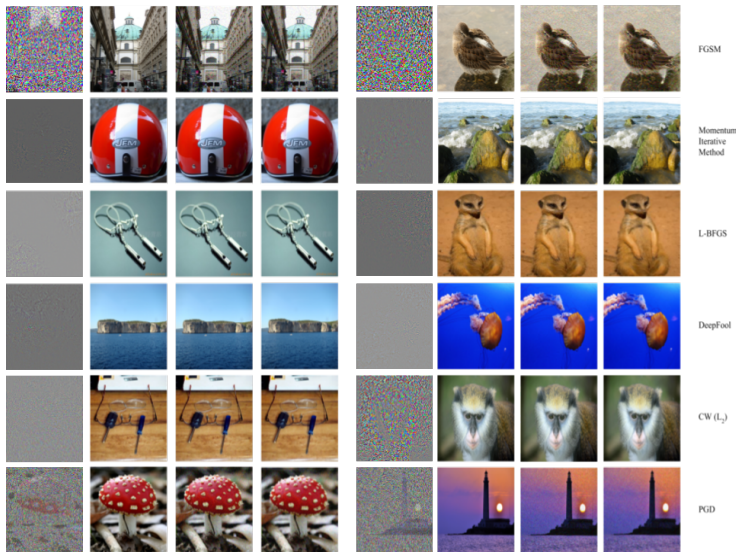


Fig. 2: The effect of bilateral filtering on adversarial inputs. From left to right, we show the adversarial perturbation, the clean image, the adversarial images generated by the respective attack algorithms, and the recovered image after bilateral filtering. Note that bilateral filtering does not destroy image quality, and images can be correctly classified.

3.3 Adaptive Filtering

One caveat to the above method, is that the parameters for the bilateral filter must be carefully chosen such that the accuracy and confidence of the classifier are preserved. Large values for the parameters σ_s and σ_r can create an excessively blurred image, and a small filter size K may capture insufficient information to remove the adversarial perturbations. With this in mind, we train a small network which will predict the parameters of the bilateral filter (K, σ_s, σ_r) for an input image. This network will serve as a cheap preprocessing step that will remove adversarial perturbations without affecting the underlying class label. In table 2 we see that the adaptive filtering approach can remove over 80% of adversarial perturbations from ImageNet images, crafted by strong first order methods. In addition, we found that we were successful in defeating the attack itself in over 95% of the test images. If the original class label cannot be recovered with certainty, than it is important that the any malicious attack not proceed unarrested. Our adaptive filtering approach ensures that an adversary is either completely defeated, or stopped from mounting targeted attacks.

3.4 Robust Denoising Network

It has been shown that under the white-box threat model, using a denoiser as the only defense is insufficient to stop the strongest adversarial attacks. A

preprocessing stage works best with transferred adversarial examples, that is, adversarial examples generated against a different classifier with no knowledge of the defense. Currently the most promising direction for training models robust to adversarial attacks is adversarial training. Despite continuing progress on both MNIST and CIFAR10, adversarial training is still very expensive, and performs worse than denoising approaches on the same datasets. We propose a combining adversarial training with our denoising approach, giving a robust, performant classifier in the context of our threat model.

Following [1,2,4], the adversarial training framework can be expressed as the following saddle point problem with model parameters θ , and input x with true label y :

$$\min_{\theta} f(x; \theta) \quad \text{where} \quad f(x; \theta) = \mathbb{E}_{(x,y) \sim D} \left[\max_{\delta} L(\theta, x + \delta, y) \right]$$

Where a solution to the inner maximization problem represents the *most* adversarial example within some perturbation budget. Solving the outer minimization problem yields a classifier which is robust to the above adversary. [1] showed that PGD could reliably solve the inner maximization problem without linearizing it, and is thus a better adversary to train against than FGSM.

We propose a modification to the above saddle point formulation which incorporates a powerful preprocessing function $BF(x)$, giving us the following

$$\min_{\theta} f(BF(x)) \quad \text{where} \quad f(x) = \mathbb{E}_{(x,y) \sim D} \left[\max_{\delta} L(\theta, x + \delta, y_{true}) \right]$$

$$BF(x) = \frac{1}{W_p} \sum_{i \in \Omega \subset x} x(i) G_s(i) G_r(x; i)$$

$$W_p = \sum_{i \in \Omega \subset x} G_s(i) G_r(x; i)$$

Here $BF(x)$ is the bilateral filter, represented as convolutions of an image patch Ω with two Gaussian kernels. The spatial and range kernels are unchanged and denoted by $G_s(\cdot)$ and $G_r(\cdot)$ respectively, weighting and normalization occur as in the vanilla bilateral filter. Because all our operations are differentiable, it is straightforward to construct a layer in a neural network to perform the bilateral filter.

Using the above brute-force formulation, the bilateral filter naturally has a $\mathcal{O}(n^2)$ cost associated with computing the response of individual pixels. Making it the most expensive operation in the graph. To reduce computation time, We choose as our preprocessing function the Permutohedral Lattice implementation of the bilateral filter [2], which is also fully differentiable and can be computed in $\mathcal{O}(n)$ time. To train our model we use the same experimental setup as in [1]. We train our model using the adversarial training framework against FGSM and PGD adversaries, and evaluate on the MNIST digits dataset, as well as CIFAR-10.

For the MNIST dataset we construct a model with two convolutional layers, with 32 and 64 filters respectively. We use 2x2 max pooling followed by a single

logit layer with 1024 units. We then prepend our bilateral filter layer to the first convolutional layer. During training we observe a faster convergence in training loss, and increased robustness to white-box FGSM, PGD, and CW attacks. In addition, we train against an FGSM adversary and show that we do similarly well against further attack. However, the model trained against FGSM does worse against stronger adversaries such as PGD, as the attack itself is a weak adversary. A model trained to be robust to FGSM will never be exposed to the small perturbations present in iterative attacks.

To test our model against CIFAR-10, we train a similar small 5 layer convolutional network with 2x2 max pooling and a final logit layer with 4096 units. In addition, we train a ResNet18 network and test both against FGSM and 20 step PGD as adversaries. We add our BF_{diff} layer to the input of our networks and train them end to end. We show that our BFNet is more robust than a standard adversarially trained model.

Because adversarial examples pose a real world risk to mission-critical AI systems, we plan to open-source our models and implementation soon. We believe it is especially important for defenses against adversarial defenses to be open and validated.

4 Experiments

4.1 Adaptive Filtering Model

In this section we show that our adaptive filtering model can correctly predict filtering parameters which will restore an adversarial input. To test this, we generate a dataset of 1000 adversarial images from five different attacks: Projected Gradient Descent with 40 steps (PGD), Box constrained L-BFGS, The Carlini & Wagner L_2 attack (CW), The Momentum Iterative FGSM (MIM), FGSM, and DeepFool

Where applicable, we constrain the perturbations to an ϵ -ball of radius 0.3 from the training example. Source images have been normalized to a range of $[-1, 1]$

Adaptive Network Architecture To build our classifier we first extract information about the distribution of pixel gradients by convolving the input with a Sobel filter in the x and y direction. Because adversarial attacks directly change values of the input, adversarial examples will often have larger color gradients in the x and y direction than natural images. We concatenate the gradient map depth-wise with the input image, and use three dilated convolutional layers with 64, 128, and 256 filters respectively, followed by 2x2 max pooling and a linear layer of 64 units. We use a dilation rate of 2 for each of the convolutional layers.

To construct our training set we use 1000 images generated from each of the attacks in table 1. For each image, we collect labels in the form of triples (K, σ_s, σ_r) , K denotes the kernel size, and σ_s, σ_r are the standard deviation for

Network	FGSM	MI-FGSM	DeepFool	CW (L_2)	L-BFGS
Inception V3	97.0	97.5	98.8	99.2	97.8
InceptionResNet V2	94.2	98.4	96.3	98.8	95.1
ResNet V2	96.5	98.0	96.1	98.1	98.0

Table 1: Recovery performance for manually chosen bilateral filter parameters. We measure recovery by the percentage of examples which, after filtering, revert to the classification label assigned to the same, unperturbed image. We use odd filter diameters of size 5, 7 and σ_s , σ_r of 0.5. This shows that with carefully chosen parameters, we can recover nearly all adversarial examples

the spatial and range kernels respectively. Given any adversarial example, there may be many permutations of parameters for the bilateral filter that successfully denoise the input. For this reason we collect a maximum of 10 different parameter configurations for each image in our training set. Given this is a multi-class prediction problem, we train using a sigmoid function at the output of our network to predict a set of candidate parameter configurations. At test time we evaluate with the parameters predicted by the maximally activated output unit. Our results are presented in tables 2, and 3.

We used the pretrained Inception V3 [2] and InceptionResNet V2 [1] ImageNet classifiers as our source networks. To generate adversarial examples on these networks, we used the open-source Cleverhans toolbox [25]. the model was trained using SGD with Nesterov momentum for 25 epochs. We then test on six different validation sets, one for each adversary respectively.

It can be seen that we recover adversarial examples generated by FGSM, PGD, CW and DeepFool near perfectly, while missing nearly 15% of the examples of MIM and L-BFGS. These results are significantly better than the results in [16], which used a 3x3 average filter to recover images. Our Adaptive Filtering network succeeds in removing adversarial examples generated on natural images, and it does so using a relatively simple method. This makes the Adaptive Filtering network a viable method for defending networks against an adversary who employs a wide range of attacks.

Source Network	Clean	FGSM	PGD	MIM	CW	DeepFool	L-BFGS
Inception V3 _A	95.0	89.0	90.7	79.1	89.1	90.3	81.3
InceptionResNet V2 _A	91.1	87.2	87.1	75.3	87.8	85.0	80.8
Inception V3 _B	95.0	95.9	98.0	96.4	94.1	95.3	96.2
InceptionResNet V2 _B	91.1	93.1	98.0	94.3	97.8	92.0	95.3

Table 2: Performance of our adaptive bilateral filter (AF) network across different attacks. We show the success rate of the top 5 parameter predictions with respect to recovering the original predicted classification label from the adversarial example (A). Note that this is with respect to the original classifier behavior, not the ground truth labels. We also show how often AF is able to defeat the adversarial attack, that is, change the classification from the adversarial label to a new one. InceptionResNet V2 is known to be a more robust network than Inception V3, hence the adversarial examples that succeed in fooling it are comparatively more robust

Network	Clean	FGSM	PGD	MIM	CW	DeepFool	L-BFGS
Inc V3 _{top1}	78.8	30.1	0.2	0.1	0.1	0.7	0.0
Inc V3 _{top5}	94.4	65.2	4.8	5.5	7.3	0.5	12.1
AF + Inc V3 _{top1}	71.7	71.0	71.6	63.1	71.1	70.1	64.2
AF + Inc V3 _{top5}	89.6	84.0	86.3	74.6	84.1	85.2	76.7
IncResNet V2 _{top1}	80.4	55.3	0.8	0.5	0.3	2.5	0.0
IncResNet V2 _{top5}	95.3	72.1	15.8	10.2	10.3	8.5	19.2
AF + IncResNet V2 _{top1}	73.1	70.1	70.8	60.5	70.3	70.5	65.0
AF + IncResNet V2 _{top5}	86.7	83.1	82.8	71.7	83.6	85.6	77.0

Table 3: Top1 and top5 accuracy of InceptionV3 and Inception-ResNetV2 on adversarial examples. Adversarial examples were generated by running the listed attacks on the ImageNet 2012 validation set. We can see that adaptive filtering significantly increases the robustness of the classifier against many diverse attacks

4.2 Robust Denoising Network

Here we show the strength of BFNet against the final adversary: one who can mount perfect knowledge attacks. For all experiments, we prepend our differentiable bilateral filtering layer to the network, and attack it by backpropagating through the entire defense. We first present our BFNet combined with robust

optimization by evaluating it with adversarial training on MNIST and CIFAR-10 datasets. We then show the robustness of BFNet without any robust optimization training methods. We will see that BFNet shows significant robustness to both L_∞ and L_2 adversaries both with and without adversarial training.

MNIST To show that BFNet is robust to strong first-order adversaries, we train a small convolutional network to 99.2% accuracy on the test set. Our vanilla model consists of 2 convolutional layers with 32 and 64 filters respectively, each followed by 2×2 max pooling and ReLU. We use a final fully connected layer with 1024 units. We modify our network into a BFNet by adding our bilateral filter layer at the input of the first convolutional layer. We then train with adversarial training using three distinct adversaries: FGSM, PGD, and PGD with the proposed CW loss function. We report the results in table 4. Our results perform well against the state-of-the-art adversarial training results. We also show that when our network is trained on a single strong adversary, we are robust to attacks from other adversaries.

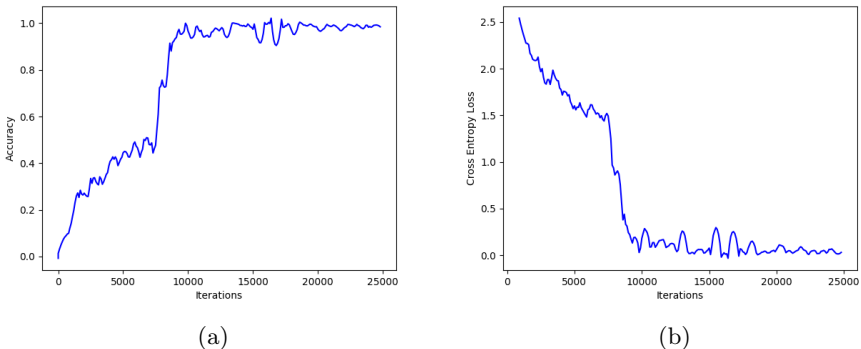


Fig. 3: The average mini-batch batch accuracy (a) and cross entropy loss (b) for the model trained with adversarial training on MNIST. We trained our model to convergence, which happened near 20k iterations. We can see that the training is stable and converges to a similar training error as a naturally trained network

Network	Clean	FGSM	PGD	CW	CW ($\kappa = 50$)
BFNet _{pgd}	99.0	95.5	98.0	93.2	-
BFNet _{fgsm}	99.0	98.1	36.4	88.2	96.0
Madry et al.	98.8	95.6	93.2	94.0	93.9
Tramer et al _A	98.8	95.4	96.4	-	95.7
Tramer et al _B	98.8	97.8	-	-	-

Table 4: Comparison of our method with state of the art adversarial training results. BFNet_{pgd} denotes our model trained against a PGD adversary, while BFNet_{fgsm} is trained against a FGSM adversary. For Tramer et al. We report A: the strongest white box attack given against a non-ensembled model from [32], as well as B: the performance of architecture B from [19]

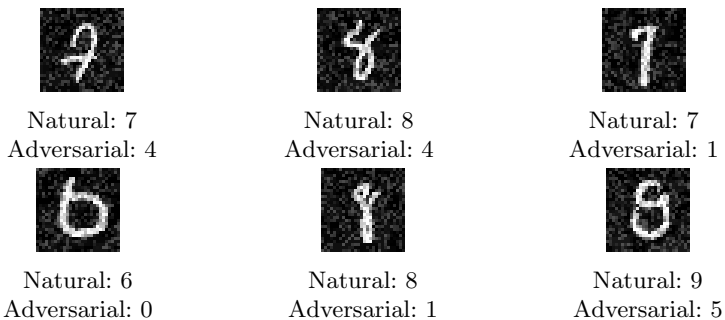


Fig. 4: PGD adversarial examples which fool an adversarially trained BF_{PGD} with $\epsilon = 0.3$

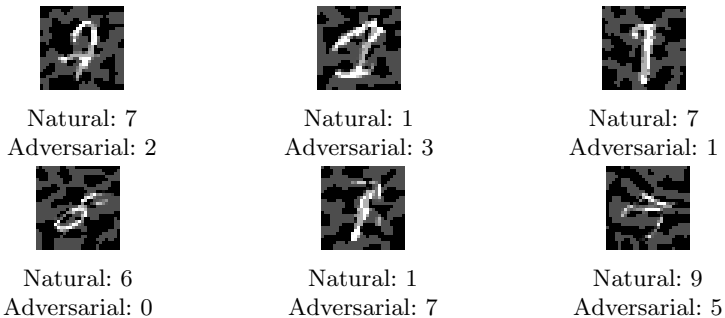


Fig. 5: FGSM adversarial examples which fool adversarially trained BF_{fgsm} with $\epsilon = 0.3$

CIFAR10 We perform similar experiments to test BFNet on CIFAR-10. Primarily we use a network with four convolutional layers, each followed by 2x2 max pooling. We use a wide linear layer of 4096 units before softmax. As with our MNIST experiments, we add a differentiable bilateral filter layer to the beginning of the network. When naturally trained with Adam for 30 epochs, this network reaches an accuracy of 79.04% on the test set. We also train the original ResNet-18 model used in [19] for 80K iterations. Trained on natural samples we reach an accuracy of 92.7% on the test set. Each model is trained adversarially with PGD and FGSM. We use an L_∞ bound of $\epsilon = 8$ for both adversaries. We use 20 step PGD with a learning rate of 2.0. We report our results in table 5

Method	Network	Clean	FGSM	PGD
BFNet _{pgd}	A	87.1	55.2	50.4
BFNet _{pgd}	B	73.1	64.5	38.1
BFNet _{fgsm}	B	76.5	70.6	12.2
Madry et al.	C	87.3	56.1	45.6

Table 5: Performance of our two adversarially trained BFNets. BF_{pgd} denotes our model trained against a PGD adversary, while BFNet_{fgsm} is trained against a FGSM adversary. Network (A) refers to the ResNet style network, while (B) refers to the smaller architecture. (C) denotes architecture (A) from [19]

4.3 ImageNet

Due to the high cost of adversarial training on natural images, we test robustness of ImageNet classifiers when they are modified *only* with a bilateral filter layer at the input. We use this as an opportunity to test the robustness of BFNet that cannot be attributed to adversarial training. To this end, we use the Inception V3 and the Inception-ResNet V2 networks, and add our bilateral filter layer to the input, keeping the pretrained ImageNet weights. We test against both L_2 and L_∞ adversaries to obtain a complete picture of BFNet’s robustness. L_∞ is a more informative metric when discussing the magnitude of adversarial attacks on very small images, because a large perturbation measured under the L_∞ norm equates to a large visual change across few pixels. But with larger, natural images, a perturbation with a large L_∞ distance is less interpretable. A large change to a single pixel may still go unnoticed to a human observer, while a large perturbation under the L_2 norm gives more information about the *total distortion* caused by the adversarial attack.

Fig. 6: Comparison of adversarial images created with BFNet vs a vanilla unmodified classifier



(a) Adversarial images generated with DeepFool on a vanilla Inception V3 classifier. The adversarial images are visually identical to the real images, and have an average L_2 norm of 0.09



(b) Adversarial examples generated by an L-BFGS adversary on a vanilla Inception V3 classifier. The adversarial examples have an average L_2 distance of 0.025 from their natural counterparts, and have visually imperceptible perturbations.



(c) Adversarial examples generated by L-BFGS on a BFNet version of the Inception V3 classifier. Generated adversarial examples have visually identifiable perturbations, and have an average L_2 norm of 106.2



(d) Adversarial examples generated by DeepFool on a BFNet version of the Inception V3 classifier. The generated adversarial examples have large, noisy perturbations, and have an average L_2 norm of 181.2

4.4 L_2 Robustness

To measure resistance to attacks under the L_2 norm, we use the unbounded attacks L-BFGS and DeepFool. It is impossible to be fully resistant to unbounded attacks, because any image can be changed to a completely different image as long as there is no bound on the size of the perturbation. In this case, we report the average L_2 and L_∞ distance of the generated adversarial images from the unbounded attacks.

We can see that our approach yields a very robust model against adversarial perturbations under the L_2 metric. When attacking our BFNet models with DeepFool, we see that the generated adversarial image has an L_∞ distance over $30x$ larger, when compared to an unmodified network of the same architecture. Similarly, we can see that the L_2 distance of an adversarial generated against BFNet is far larger when compared to adversarial images generated against a network of the same architecture without the bilateral filter. With respect to the L-BFGS attack, we see a similarly large disparity between BFNet and a vanilla network.

Network	L_∞	L_2
Inception V3 _{Natural}	0.015	0.43
Inception V3 _{BFNet}	0.621	148.29
IncResNet V2 _{Natural}	0.025	0.44
IncResNet V2 _{BFNet}	0.793	187.45

Table 6: Performance of BFNet against the unbounded DeepFool attack. We report the average L_2 and L_∞ distance of 1000 adversarial images on Inception V3 and Inception-ResNet V2.

Network	L_∞	L_2
Inception V3 _{Natural}	0.02	0.67
Inception V3 _{BFNet}	0.39	90.52
IncResNet V2 _{Natural}	0.06	0.77
IncResNet V2 _{BFNet}	0.65	90.65

Table 7: Performance of BFNet against unbounded L-BFGS attack. We report the average L_2 and L_∞ distance of 1000 adversarial images on Inception V3 and Inception-ResNet V2.

4.5 L_∞ Robustness

For the L_∞ attacks such as FGSM, and MI-FGSM we measure the resistance of our model to different values of perturbation ϵ . We can see that our BFNet significantly decreases the attack strength of L_∞ adversaries, in most cases by over 50%. Of particular note is that we show more significant resistance to adversarial perturbations of $\epsilon \leq 0.3$. Larger perturbations are visually discernible, and thus are less adversarial than smaller fooling perturbations. For both attacks we use 1000 random images sampled from the ILSVRC 2012 validation set, and report the percentage of successful attacks against both the natural model, and the BFNet modified network for a wide range of epsilon values.

Network	Epsilon	Natural	BFNet
Inception V3	0.1	73.2	30.2
Inception V3	0.15	78.6	36.6
Inception V3	0.3	93.2	46.6
Inception V3	0.5	99.0	63.2
Inception V3	0.75	100.0	90.8
Inception V3	1.0	100.0	99.8
IncResNet V2	0.1	58.8	42.6
IncResNet V2	0.15	65.6	55.4
IncResNet V2	0.3	88.2	75.4
IncResNet V2	0.5	98.0	91.0
IncResNet V2	0.75	99.6	99.6
IncResNet V2	1.0	99.6	99.6

Table 8: Performance of BFNet against an FGSM adversary for a range of perturbation sizes (lower is better)

Network	Epsilon	Natural	BFNet
Inception V3	0.1	58.8	21.0
Inception V3	0.15	65.6	30.1
Inception V3	0.3	88.2	42.2
Inception V3	0.5	98.0	52.4
Inception V3	0.75	99.6	53.4
Inception V3	1.0	99.6	70.8
IncResNet V2	0.1	89.1	59.0
IncResNet V2	0.15	90.6	38.6
IncResNet V2	0.3	92.2	59.4
IncResNet V2	0.5	100.0	74.6
IncResNet V2	0.75	100.0	80.2
IncResNet V2	1.0	100.0	91.8

Table 9: Performance of the BFNet against an MI-FGSM adversary. We again report the performance of BFNet against an unmodified network for a variety of values of epsilon. For our MI-FGSM attack, we use a momentum decay factor of 1.0, and run the attack for 10 iterations

Conclusion

The continued existence of adversarial examples, and the lack of effective defenses limits our ability to deploy AI systems in critical areas where safety and security are necessary. Here we showed that a bilateral filter can be used as the core of versatile, effective defenses to recover clean images before classification. The bilateral filter remains effective when deployed with numerous defense strategies: as a manual preprocessing step, a trained denoiser, or a robust model that’s trained end-to-end. As the attacker grows in knowledge of our defense, as well as employs stronger algorithms, our defense holds.

Because the bilateral filter encourages piecewise smoothness, we see that the bilateral filter effectively projects adversarial images back to the distribution of natural images. Furthermore, when trained end to end, our bilateral filter can be combined with adversarial training approaches to create a robust defense method. In the future we hope to see preprocessor defenses tested by direct white-box attack, and combined with robust optimization methods like adversarial training to create performant, unified defenses.

References

1. A. Adams, J. Baek, and M. A. Davis. Fast high-dimensional filtering using the permutohedral lattice. *Computer Graphics Forum*, 29(2):753762, 2010.
2. Anish Athalye, Nicholas Carlini, and David Wagner. Obfuscated gradients give a false sense of security: Circumventing defenses to adversarial examples. *arXiv preprint arXiv:1802.00420*, 2018.
3. Nicholas Carlini, and David Wagner. MagNet and Efficient Defenses Against Adversarial Attacks are Not Robust to Adversarial Examples. *arXiv preprint arXiv:1711.08478*, 2017
4. Nicholas Carlini and David Wagner. Towards evaluating the robustness of neural networks. *arXiv preprint arXiv:1608.04644*, 2016.
5. Nicholas Carlini and David Wagner. Adversarial examples are not easily detected: Bypassing ten detection methods. *arXiv preprint arXiv:1705.07263*, 2017.
6. Nilaksh Das, Madhuri Shanbhogue, Shang-Tse Chen, Fred Hohman, Li Chen, Michael E. Kounavis, and Duen Horng Chau. Keeping the Bad Guys Out: Protecting and Vaccinating Deep Learning with JPEG Compression *arxiv preprint arXiv:1705.02900*, 2017.
7. Yinpeng Dong, Fangzhou Liao, Tianyu Pang, Hang Su, Xiaolin Hu, Jianguo Li, and Jun Zhu. Boosting Adversarial Attacks with Momentum *arxiv preprint arXiv:1710.06081*, 2017.
8. G. K. Dziugaite, Z. Ghahramani, and D. M. Roy. A study of the effect of jpg compression on adversarial images. *arXiv preprint arXiv:1608.00853*, 2016.
9. Ivan Evtimov, Kevin Eykholt, Earlene Fernandes, Tadayoshi Kohno, Bo Li, Atul Prakash, Amir Rahmati, and Dawn Song. Robust physical-world attacks on deep learning models. *arXiv preprint arXiv:1707.08945*, 2017.
10. Ian J. Goodfellow, Jonathon Shlens, and Christian Szegedy. Explaining and harnessing adversarial examples. *arXiv preprint arXiv:1412.6572*, 2014.
11. Alex Krizhevsky. Learning Multiple Layers of Features from Tiny Images. Masters thesis, 2009.
12. Alex Krizhevsky, I. Sutskever, and G. E. Hinton. Imagenet classification with deep convolutional neural networks. In *Advances in neural information processing systems*, pages 10971105, 2012.
13. A. Kurakin, I. Goodfellow, and S. Bengio. Adversarial examples in the physical world. *arXiv preprint arXiv:1607.02533*, 2016.
14. Xin Li and Fuxin Li. Adversarial Examples Detection in Deep Networks with Convolutional Filter Statistics. *arXiv preprint arXiv:1612.07767*, 2016

15. Bin Liang, Hongcheng Li, Miaoqiang Su, Xirong Li, Wenchang Shi and Xiaofeng Wang. Detecting Adversarial Image Examples in Deep Neural Networks with Adaptive Noise Reduction. *arXiv preprint arXiv:1705.08378*, 2018
16. Fangzhou Liao, Ming Liang, Yinpeng Dong, Tianyu Pang, Jun Zhu, and Xiaolin Hu Defense against Adversarial Attacks Using High-Level Representation Guided Denoiser. *arXiv preprint arXiv:1712.02976*, 2017
17. Y. Luo, X. Boix, G. Roig, T. Poggio, and Q. Zhao. Foveation-based mechanisms alleviate adversarial examples. *arXiv preprint arXiv:1511.06292*, 2015.
18. C. Lyu, K. Huang, and H.-N. Liang. A unified gradient regularization family for adversarial examples. In *Data Mining (ICDM), 2015 IEEE International Conference on*, 2015, pp. 301309.
19. Aleksander Madry, Aleksandar Makelov, Ludwig Schmidt, Dimitris Tsipras and Adrian Vladu Towards Deep Learning Models Resistant to Adversarial Attacks *arXiv preprint arXiv:1706.06083*, 2017
20. Dongyu Meng and Hao Chen. MagNet: a Two-Pronged Defense against Adversarial Examples. In *ACM Conference on Computer and Communications Security (CCS)*, 2017.
21. S. M. Moosavi-Dezfooli, A. Fawzi, O. Fawzi, and P. Frossard. Universal adversarial perturbations. In *CVPR*, 2017.
22. S.-M. Moosavi-Dezfooli, A. Fawzi, and P. Frossard. Deepfool: A simple and accurate method to fool deep neural networks. In *CVPR*, 2016.
23. N. Papernot, P. McDaniel, I. Goodfellow, S. Jha, Z. B. Celik, and A. Swami. Practical black-box attacks against machine learning. In *Proceedings of the 2017 ACM on Asia Conference on Computer and Communications Security*, ASIA CCS 17, pages 506519, 2017.
24. Nicolas Papernot and Patrick D. McDaniel. On the effectiveness of defensive distillation. *arXiv preprint arXiv:1607.05113*, 2016.
25. Nicolas Papernot, Nicholas Carlini, Ian Goodfellow, Reuben Feinman, Fartash Faghri, Alexander Matyasko, Karen Hambardzumyan, Yi-Lin Juang, Alexey Kurakin, Ryan Sheatsley, Abhibhav Garg, and Yen-Chen Lin. Cleverhans v2.0.0: an adversarial machine learning library. *arXiv preprint arXiv:1610.00768*, 2017.
26. N. Papernot, P. McDaniel, X. Wu, S. Jha, and A. Swami. Distillation as a defense to adversarial perturbations against deep neural networks. In *IEEE Symposium on Security and Privacy*, pages 582597, 2016.
27. N. Papernot, P. D. McDaniel, S. Jha, M. Fredrikson, Z. B. Celik, and A. Swami. The limitations of deep learning in adversarial settings. In *IEEE European Symposium on Security and Privacy, EuroS&P 2016, Saarbrücken, Germany, March 21-24, 2016*, pages 372387, 2016.

28. Pouya Samangouei, Maya Kabkab and Rama Chellappa Defense-GAN: Protecting Classifiers Against Adversarial Attacks Using Generative Models In *International Conference on Learning Representation*, 2018.
29. Uri Shaham, Yutaro Yamada, and Sahand Negahban. Understanding adversarial training: Increasing local stability of neural nets through robust optimization. *arXiv preprint arXiv:1511.05432*, 2015. Available on OpenReview <https://openreview.net/forum?id=BkJ3ibb0>
30. Shiwei Shen, Guoqing Jin, Ke Gao, and Yongdong Zhang. APE-GAN: Adversarial Perturbation Elimination with GAN *arXiv preprint arXiv:1707.05474*, 2017.
31. C. Szegedy, G. Inc, W. Zaremba, I. Sutskever, G. Inc, J. Bruna, D. Erhan, G. Inc, I. Goodfellow, and R. Fergus. Intriguing properties of neural networks. In ICLR, 2014.
32. Florian Tramr, Alexey Kurakin, Nicolas Papernot, Dan Boneh, and Patrick D. McDaniel. Ensemble adversarial training: Attacks and defenses. *arXiv preprint arXiv:1705.07204*, 2017.
33. Christian Szegedy, Sergey Ioffe, Vincent Vanhoucke and Alex Alemi Inception-v4, Inception-ResNet and the Impact of Residual Connections on Learning. *arXiv preprint arXiv:1602.07261*, 2016.
34. Florian Tramr, Nicolas Papernot, Ian J. Goodfellow, Dan Boneh, and Patrick D. McDaniel. The space of transferable adversarial examples. *arXiv preprint arXiv:1704.03453*, 2017.
35. Christian Szegedy, Vincent Vanhoucke, Sergey Ioffe, Jonathon Shlens, and Zbigniew Wojna Rethinking the Inception Architecture for Computer Vision *arXiv preprint arXiv:1512.00567*, 2015.
36. Weilin Xu, David Evans, and Yanjun Qi. 2017. Feature Squeezing: Detecting Adversarial Examples in Deep Neural Networks. *arXiv preprint arXiv:1704.01155*(2017).